Fine Structure and Dynamics of the Solar Atmosphere
Proceedings IAU Symposium No. 327, 2016
S. Vargas Domínguez, A.G. Kosovichev, P. Antolin & L. Harra, eds.

doi:10.1017/S174392131700401X

P-mode induced convective collapse in vertical expanding magnetic flux tubes?

D. Utz[1,2], T. Van Doorsselaere[2], N. Magyar[2], M. Bárta[3] and J. I. Campos Rozo[4]

[1]IGAM, Institute of Physics, Karl-Franzens University Graz, Universitätsplatz 5II, AT-8010, Graz, Austria
email: dominik.utz@uni-graz.at

[2]Centre for mathematical Plasma Astrophysics, KU Leuven, Celestijnenlaan 200B, bus 2400, B-3001, Leuven, Belgium
email: tom.vandoorsselaere@kuleuven.be

[3]Astronomical Observatory of the Czech Academy of Sciences, Fričova 298, Cz-251 65, Ondřejov, Czech Republic
email: miroslav.barta@asu.cas.cz

[4]National Astronomical Observatory of Colombia, National University of Colombia, Carrera 30 #45-03 ed. 413, Bogota, Colombia
email: jicamposr@unal.edu.co

Abstract. Small-scale kG strong magnetic field elements in the solar photosphere are often identified as so-called magnetic bright points (MBPs). In principle these MBPs represent the cross-section of a vertical, strong, magnetic flux tube which is expanding with height in the solar atmosphere. As these magnetic elements represent possible MHD wave guides, a significant interest has been already paid to them from the viewpoint of observations and simulations. In this work we would like to shed more light on a possible scenario for the creation of such strong magnetic field concentrations. The accepted standard scenario involves the convective collapse process. In this ongoing work we will show indications that this convective collapse process may become triggered by sufficiently strong pressure disturbances. However, it is highly unlikely that p-mode waves can be of such a strength.

Keywords. magnetic flux tubes, MHD-simulation, convective collapse, p-mode waves

1. Introduction

A very important constituent of the solar magnetic field is the magnetic network on the boundaries of the supergranular cells. Within this magnetic network one can often identify small-scale strong magnetic field concentrations as they show up brighter than their surrounding. Such so-called magnetic bright points (MBPs) are thought to be the cross sections of kG strong magnetic flux tubes with diameters of just a few hundred km in the solar photosphere (see, e.g., Borrero *et al.* 2015, for a recent review). Due to their strong magnetic fields and their tube-like topology, they are suitable candidates for guiding MHD waves from the lower solar atmosphere into the higher atmosphere where these waves can then be scattered, reflected, damped, and finally absorbed and thus contribute to the coronal heating (e.g., Mathioudakis *et al.* 2013).

The creation of these strong flux tube elements is thought to be due to the convective collapse process in which a strong enough magnetic field concentration leads to a lowering of the temperature inside the concentration. This is due to the inhibition of the convective energy transport inside the flux tube which can then not counterbalance anymore the radiative losses. The lower temperature leads ultimately to a higher density which then

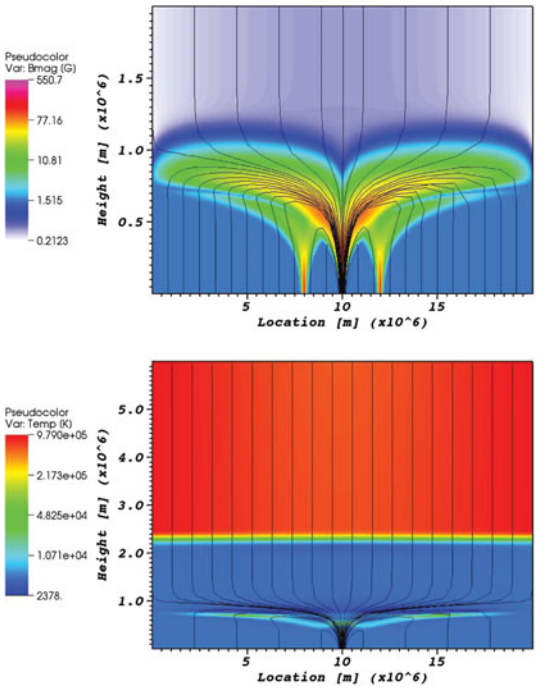

Figure 1. Top: the effective ($\sqrt{B_x^2 + B_z^2}$) magnetic field configuration of the test solar atmosphere consisting of one strong positive flux element in the centre and two parasitic weaker magnetic flux elements to each side. Bottom: the corresponding self-consistent solution for the temperature field of this flux tube atmosphere embedded in a stratified background atmosphere.

triggers and initiates a downflow inside the flux tube and hence an evacuation of the flux tube structure starts. The evacuated structure cannot withstand the outside plasma pressure anymore and collapses under the surrounding pressure. As this process happens on very short time-scales, it is known as convective collapse (for the theory see, e.g., Spruit 1979 and for the observational verification, e.g., Nagata *et al.* 2008).

The question we raise in this contribution and wish to answer is, what process triggers the convective collapse. A possible scenario is outlined in Kato *et al.* (2011) where the authors propose the so-called magnetic pumping process under which one can understand that granular convective downflows on the outside of an existing flux tube massage the flux element in such a way as to push also the plasma down inside the element. This pumping process leads subsequently also to the creation of upwards traveling slow mode waves when the atmosphere rebounds.

Contrary to this mechanism we would like to test in this ongoing work if the pressure change below a magnetic flux tube induced by a passing p-mode wave would be sufficient to initiate the convective collapse process.

2. The MHD model setup

To test the hypothesis that p-modes could act as a trigger for the convective collapse observed in small-scale magnetic fields, we set up a numerical model.

The used simulation tool and the implemented physics. For our simulations we use the numerical MHD code MPI-AMRVAC (Message Passing Interface - Adaptive Mesh Refinement Versatile Advection Code), which was developed, maintained, and is still hosted

https://doi.org/10.1017/S174392131700401X Published online by Cambridge University Press

at KU Leuven. More details about the code can be found, e.g., in Porth *et al.* (2014), as well as under `http://homes.esat.kuleuven.be/~keppens/`.

We run the code in the ideal MHD setup (no resistivity and no viscosity) with a full energy equation treatment, i.e., non isothermal and non polytropic, but without heat conduction and or radiative effects (there is no radiation treatment).

The solar background atmosphere. The background atmosphere is modeled in a simpler fashion than usual, which means that instead of employing, e.g., the VAL-C model atmosphere (e.g., by look-up tables), we model the temperature profile from the photosphere to the corona by three isothermal layers which are connected by two hyperbolic tangent functions to avoid discontinuities. After setting up the temperature profile within the simulation box the density and pressure profiles can be calculated by the barometric scale height equation and the ideal gas law under the consideration that the scale height parameter is changing within the domain due to the changing temperature profile. For the full details we refer to Utz *et al.* (2017).

The flux tube atmosphere. The magnetic field configuration of our atmosphere can be built by the superposition of isolated single flux elements. For that purpose we started with a given horizontal profile for the vertical magnetic field strength modeled via a Gaussian. This horizontal profile is expanded following a tanh function with height (modelling the opening of the flux tube due to the decreasing gas pressure with height). The horizontal magnetic field component can be found via the divergence-free constraint of the magnetic field. As the divergence operator is linear we can use the superposition principle to add up several divergence free magnetic flux tubes. For details of our flux tube modelling we also refer to Utz *et al.* (2017). In the current work we used 3 flux tubes with a strong positive polarity one (550 G magnetic field strength in the core) centred in the domain with about 120 km in diameter (FWHM) and two parasitic ones with opposite field strengths of nearly 140 G positioned 2 Mm far away to the left and to the right (roughly two granular diameters). The flux tubes expand in such a way that the magnetic canopy is established at a height of roughly 800 km. A visualisation of this initial magnetic flux tube atmosphere can be found in Fig. 1, upper panel.

Achieving magneto-static conditions in an arbitrary magnetic field configuration. After the creation of the background atmosphere and the modelling of the magnetic field within the numerical box, an important and quite complicated task is to find magnetostatic initial solutions, i.e. one needs to adjust the background atmosphere (pressure, temperature, density) in such a way as to become force-free together with the newly prescribed magnetic fields. This is especially important if one is interested in wave creation and propagation processes. In our case we followed the approach outlined in detail in the before cited work of Utz *et al.* (2017). A very similar approach is described in the works of Gent *et al.* (2013) and Gent *et al.* (2014). In our approach the principle idea is that the gradient in the horizontal pressure (and thus an induced horizontal force) is adjusted in exactly such a way as to compensate the effective horizontal Lorenz force component coming from the magnetic pressure as well as the magnetic tension force. To compensate for the vertical Lorenz force component one can adjust the density in a gravitationally stratified atmosphere (see Fig. 2, top panel for the density stratification). By applying these two steps within the numerical box automatically also the temperature gets adjusted as a byproduct due to the constraint of the ideal gas law (see e.g. Fig. 1, lower panel). To achieve a good force balance small-scales need to be resolved. Thus we used an adaptive mesh refinement which resolves up to a level of 5 km in the horizontal direction and 3 km in the vertical one as can be seen in Fig. 2, lower panel.

https://doi.org/10.1017/S174392131700401X Published online by Cambridge University Press

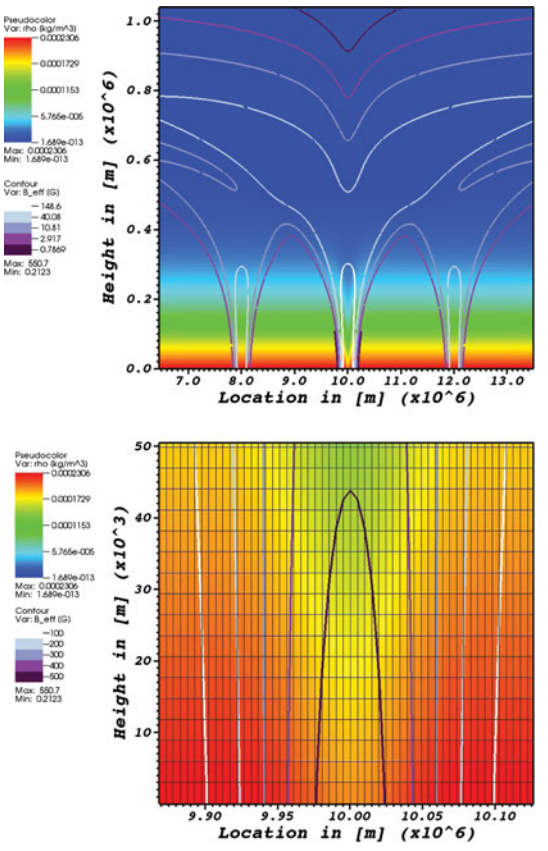

Figure 2. Top: the self-consistent density stratification for the magnetic field configuration as shown in Fig. 1. Bottom: a small detail of the inside of the flux tube illustrating the highest achieved resolution via the adaptive mesh refinement which refines the cells up to 5 km in the horizontal and 3 km in the vertical dimension. The contours give the effective magnetic field strength and thus roughly the shape of the flux tube.

3. Driving the simulation and results

We drive our simulation in the bottom boundary by changing the gas pressure according to a p-mode. In this first approach and results of the ongoing work we have chosen to simulate only an oscillatory boundary and thus a standing wave instead of a running wave-train (i.e. a pressure disturbance on the lower boundary running from the left border of the domain to the right border of the numerical box) for simplicity of the set-up. In the near future this will be an important point of improvement to further enhance the realism of the simulation. Thus we introduced currently only a standing wave below the flux tube element with a small amplitude of about 2% of the initial pressure outside of the flux element. The density is adjusted via the adiabatic law (within the bottom boundary) meaning that the slight changes in pressure also lead to small changes in density. When we do not consider anything else, such slight disturbances would only lead to marginal contractions of the magnetic field, no significant flows, and neither strong magnetic field changes (similar conclusions can be also drawn from a first principle analysis; see the Appendix).

Thus in a second step we add artificially the effect of radiative loses (which are not treated by the code) by assuming that a less dense core of the magnetic field structure

https://doi.org/10.1017/S174392131700401X Published online by Cambridge University Press

would permit the radiation to escape more easily (lower opacity) and thus reducing the temperature and pressure inside of the flux tube. Hence, when the density becomes smaller than the unperturbed quantity, we additionally decrease the basic initial pressure level in the boundary under the flux tubes. Moreover, we take into account the amplitude steepening of a pressure wave when running through the rarefied flux element. Thus the lower boundary condition for pressure and density looks like:

$$p = p_0 + A \cdot p_0 \sin(2\pi t/T) \cos(2\pi(x - x_0)/w)\rho_0/\rho(x, y + \Delta y, t);\ \rho = \rho_0 \cdot (p/p_o)^{(3/5)}, \quad (3.1)$$

where p_0 stands for the initial unperturbed gas pressure, A the amplitude of the pressure wave (0.02), T the the period (300 s), x_0 the position of the flux tube relative to the left boundary (10^7 m), w the spatial extension of the p-mode (10^6 m), and $\rho_0/\rho(x, y + \Delta y, t)$ ensures that the wave amplitude becomes amplified or damped when the wave starts in a rarefied or overdense environment. In the case that the medium becomes rarefied $\rho(x, y, t)/\rho_0 < 1$ the equation for the pressure becomes slightly modified, namely the first p_0 term gets replaced by:

$$\widetilde{p_0} = p_0 \exp(-k_c \bmod(t, T/2)/\beta), \quad (3.2)$$

to mimic the additional radiative loses. Here β represents the plasma beta (in our case ~ 10) and k_c an auxiliary cooling coefficient chosen in such a way that e.g., the pressure is decreased by 10% after half of a minute (see also Appendix) yielding a value of about 0.035 for k_c. In this second case a convective collapse starts to develop, visible as fast downflows, shrinkage of the flux tube diameter, and ultimately leading also to an increase in the magnetic field strength (see plot series in Fig. 3; showing the magnetic field strength, vertical and horizontal velocity along a horizontal cut through the magnetic flux tube element just above the boundary layer). Interestingly, after a whole period of 300 s, the magnetic elements (the core one, as well as the two parasitic side ones) have settled roughly back to their initial stage.

4. Discussion and conclusion

Although our driver might not be fully realistic (e.g. the relative pressure amplitude is unrealistically high, see Appendix), the evolving scenario features several of the well observed characteristics of a convective collapse as there are the strong downflows (which are in our case even partly too strong), the shrinkage of the flux tube diameter, and the strong increase in the magnetic field (roughly doubling in value). Probably in a more realistic scenario the magnetic pumping mechanism is acting in addition and thus increasing the sidewards pressure on the flux tube, strengthening the shrinkage, and reducing the necessary downflows to achieve the strong collapse, which were in our case by a factor of 2 to 3 stronger than normally observed (see, e.g., Utz *et al.*2014). In the future we wish to investigate in addition in full detail the upwards propagating shocks and waves caused by these disturbances and have a detailed look into how they interact with the magnetic canopy layer and the corona. A nice feature of p-modes as triggers for convective collapses of small-scale magnetic fields would be the possible explanation of recurring MBPs in the same location after several minutes (see Bodnárová *et al.* 2014), e.g. by a different p-mode wave-train running through the existing magnetic field patch.

Acknowledgements

This research received support by the Austrian Science Fund (FWF): P27800. Additional funding was possible through an Odysseus grant of the FWO Vlaanderen, the IAP P7/08 CHARM (Belspo), and GOA-2015-014 (KU Leuven). N.M. acknowledges the Fund

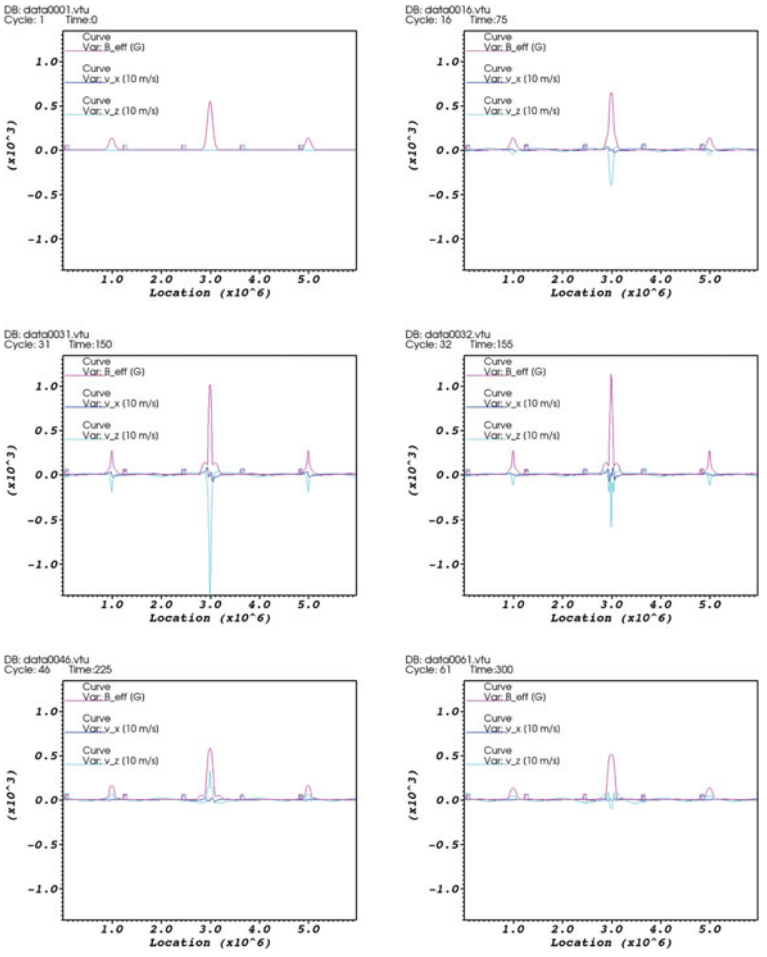

Figure 3. plot series showing the evolution of important quantities via a horizontal cut at the lower boundary of the numerical domain, namely the magnetic field strength (purple), horizontal velocities (blue), and vertical velocities (cyan). Here the velocities are depicted in units of 10 m/s. The time evolution goes from left top to right bottom with the 3rd panel showing the time step where the magnetic field reaches its maximum value during the evolution with about 1.1 kG roughly doubling the initial magnetic field strength of the flux tube.

for Scientific Research-Flanders (FWO-Vlaanderen). J. I. Campos Rozo is grateful to the National University, the Research Direction and the National Astronomical Observatory of Colombia for providing him with a travel grant under the project for new professors and researchers to spend a part of his master thesis time at KU Leuven.

5. Appendix

In this short appendix we wish to outline the possibility of p-mode induced convective collapses by a first principle analysis. Assuming that the wave processes are fast enough to be of adiabatic form we will obtain the following temperature and density changes due to the passing wave-train:

$$T_2 = T_1 \cdot \left(\frac{p_2}{p_1}\right)^{\frac{\kappa-1}{\kappa}}, \tag{5.1}$$

https://doi.org/10.1017/S174392131700401X Published online by Cambridge University Press

where p_2 and p_1 are the pressures at the p-mode minimum and the non-disturbed background pressure, T_2 and T_1 represent the temperature at the p-mode minimum and the non-disturbed background temperature, and finally κ would be the adiabatic coefficient amounting to ~ 1.66 or $5/3$. The density change can be expressed in a similar way as:

$$\rho_2 = \rho_1 \cdot \left(\frac{p_2}{p_1}\right)^{\frac{1}{\kappa}}, \tag{5.2}$$

where ρ_1 and ρ_2 are the densities at the p-mode minimum and for the non-disturbed background. If one plugs in an assumed 5% change in pressure (considering the increased amplitude due to the partially evacuated state of the magnetic field concentration), the results would yield a change in density of ∼2% and ∼3% for the temperature, respectively (both values decrease). Thus we obtain already a first indication that the lower pressure will lead to downflows as the pressure (and thus also its stratification) is lowered stronger than the density (5% compared to 2%). However, this effect is not strong enough to cause massive flows and thus the convective collapse. For example, if we assume that the pressure/gravity imbalance will lead to a non-compensated effective gravitational acceleration of about 3%, which is acting for a quarter of a period of the 5 min oscillation (one quarter of the period accelerating, one quarter decelerating, and then accelerating and decelerating in the opposite direction), we would end up with speeds of less than 0.7 km/s.

This picture changes dramatically if we consider the effect of radiative transport on first principles. A change in temperature of 3% leads via the Stefan-Boltzmann law (constant$\cdot\sigma\cdot T^4$) to a lowering of the incoming radiative flux into the flux tube atmosphere from the surface of about 12%. Thus there is now an additional imbalance in the radiative flux as the atmosphere radiates still the same amount but gets heated from below by a 12% reduced input flux.

Calculating now the energy content and the cooling rate on a first principle basis we will be able to show that the additional radiative effects will enable the observed strong downflows and the on-set of the collapse process.

The internal energy of a gas is given by:

$$U = N\frac{f}{2}k_B T, \tag{5.3}$$

where N is the number of particles, f is the degree of freedom (3 translation motions for atoms), k_B the Boltzmann constant, and T the temperature. We rewrite this equation now into the form of an energy per unit surface element by replacing N, the number of particles, by ρ and by integrating furthermore over a certain height l representing the lower atmosphere (assuming that all quantities within this height are constant). By doing so we end up with the following expression for the energy per surface element (U_A):

$$U_A = \frac{\rho N_a}{\mu} l \frac{f}{2} k_B T, \tag{5.4}$$

where ρ is the density, N_a is the Avogadro constant or Loschmidt number, and μ the atomic mass in units of g/mol. Inserting typical values for the lower solar atmosphere and keeping in mind the right units we end up with a value of roughly $1.25 \cdot 10^{12}$ erg/cm^2 ($l = 100\ km$, $\rho = 2 \cdot 10^{-7}\ g/cm^3$, $T = 5000\ K$, $\mu = 1$).

Calculating the radiative energy flux for a temperature of 6000 K with the Stefan-Boltzmann law we end up with a value of roughly $7 \cdot 10^{10}$ erg/(cm^2 s). Thus in a time as short as ∼ 20 s the whole lower (assumption 100 km thick) atmosphere would cool down, if there is no incoming flux from below. In our case, with the reduced radiative

https://doi.org/10.1017/S174392131700401X Published online by Cambridge University Press

flux, it means that after roughly half a minute the inner energy, and thus the pressure of the atmosphere above, should have dropped by an additional 15%. Thus we will get an average pressure/gravity imbalance of more than 15% within half a minute and hence effective accelerations of about 40 m/s^2. Thus after another minute, downflows of about 2.5 km/s should have evolved. Such downflows are indeed observed as well as they evolve in such time-scales (e.g., Utz *et al.* 2014).

The final question to be answered is, if the assumed 2 to 5% relative pressure amplitude for p-modes is realistic?

We start with the velocity amplitudes of single p-modes on the solar surface, which are on the order of 20 cm/s (see, e.g, Gelly *et al.* 1997, Fig. 1), to calculate the pressure amplitude of these waves:

$$p_A = v_A \rho c, \tag{5.5}$$

where p_A is the pressure amplitude, v_A the velocity amplitude, ρ the density, and c the sound speed. This equation can be brought in the following form by replacing c and writing p_A as a ratio to p_0 the background pressure (κ being the adiabatic exponent):

$$\frac{p_A}{p_0} = v_A \sqrt{\frac{\kappa \rho}{p_0}}. \tag{5.6}$$

With typical values for the solar surface, $v_A = 20$ cm/s, $\kappa = 1.66$, $p_0 = 3 \cdot 10^4\ dyn/cm^2$, and $\rho = 2 \cdot 10^{-7}\ g/cm^3$, we end up with a pressure relative amplitude of roughly $6 \cdot 10^{-5}$. Thus the assumed 2% amplitude of the initial pressure perturbation is by magnitudes too high. In fact it is by a factor of ~ 300 too high and thus even in the case of constructively interacting single p-modes (see Fig. 1 of Gelly *et al.* 1997, which shows that there are plenty of different modes available), it is highly unlikely that the pressure perturbation caused by passing p-modes could be sufficiently high to cause a convective collapse. To conclude, while an oscillatory pressure disturbance in the range of 2% should be sufficient to cause a convective collapse (shown by first principles and a simulation run above), it can be practically ruled out that passing p-mode wave-trains could create such a sufficiently strong disturbance to initiate the process as it would require in the order of 100 single p-modes to interact constructively with each other.

References

Bodnárová, M., Utz, D., & Rybák, J. 2014, *Sol. Phys.*, 289, 1543

Borrero, J. M., Jafarzadeh, S., Schüssler, M., & Solanki, S. K. 2015, *Space Sci. Rev.* .

Gelly, B., Fierry-Fraillon, D., Fossat, E., Palle, P., Cacciani, A., Ehgamberdiev, S., Grec, G., Hoeksema, J. T., Khalikov, S., Lazrek, M., Loudagh, S., Pantel, A., Regulo, C., & Schmider, F. X. 1996, *A&A* 323, 235.

Gent, F. A., Fedun, V., & Erdélyi, R. 2014, *ApJ* 789, 42.

Gent, F. A., Fedun, V., Mumford, S. J., & Erdélyi, R. 2013, *Mon. Not. R. Astron. Soc.* 435, 689.

Kato, Y., Steiner, O., Steffen, M., & Suematsu, Y. 2011, *ApJ Letter*, 730, L24

Mathioudakis, M., Jess, D. B., & Erdélyi, R. 2013, *Space Sci. Rev.* 175, 1–27.

Nagata, S., Tsuneta, S., Suematsu, Y., *et al.* 2008, *ApJ Letter*, 677, L145

Porth, O., Xia, C., Hendrix, T., Moschou, S. P., & Keppens, R. 2014, *Astrophys. J., Suppl. Ser.* 214, 4.

Spruit, H. C. 1979, *Sol. Phys.*, 61, 363

Utz, D., del Toro Iniesta, J. C., Bellot Rubio, L. R., Jurčák, J., Martínez Pillet, V., Solanki, S. K., & Schmidt, W. 2014, *ApJ* 796, 79.

Utz, D., Van Doorsselaere, T., Kühner, O., & Magyar, N, Calvo Santamaria, I., & Campos Rozo, J. I. 2016, *Cent. Eur. Astrophys. Bull.* 40, 9.

https://doi.org/10.1017/S174392131700401X Published online by Cambridge University Press